

Supporting Information for “Response of Vertical Velocities in Extratropical Precipitation Extremes to Climate Change”

Ziwei Li *, Paul O’Gorman

Department of Earth, Atmospheric and Planetary Sciences, Massachusetts Institute of Technology, Cambridge, MA, USA

*ziweili@mit.edu

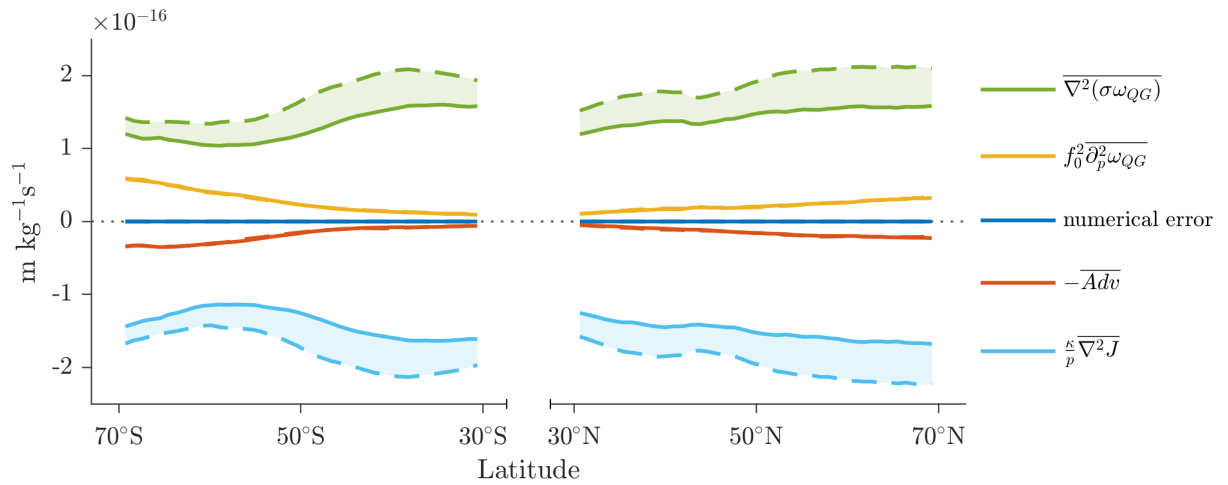


Figure S1. Event- and zonal-mean of terms in the QG- ω equation (Eq. 1) at 500hPa for extratropical precipitation extremes in CESM-LE. Solid lines indicate historical, dashed lines indicate RCP8.5, and shading indicates the response to climate change. Terms on the right-hand side of the equation are shown with a minus sign so that the sum is zero. The darker blue line gives the error in the numerical solution of the QG- ω equation.

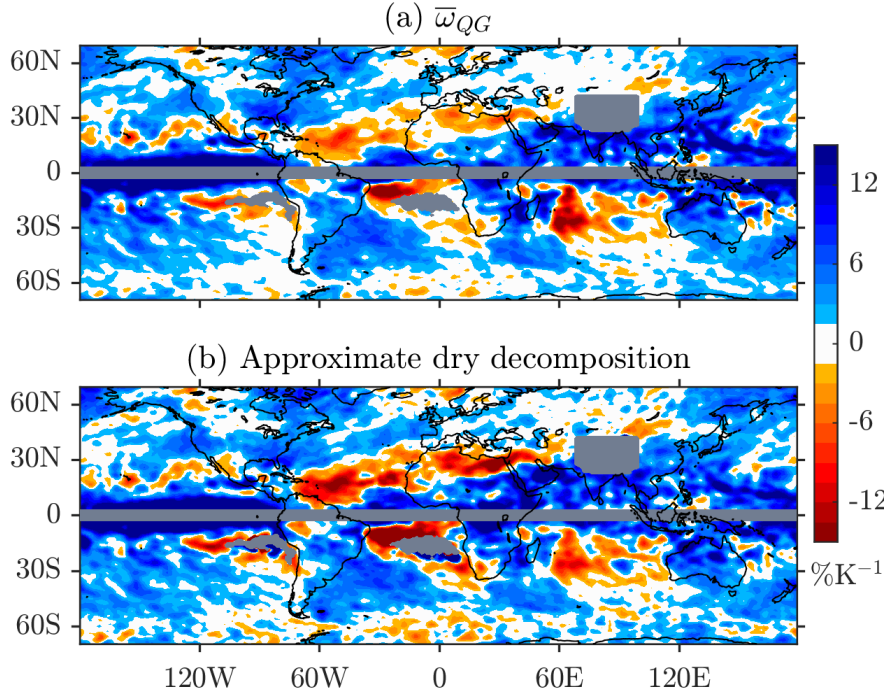


Figure S2. Changes in $\bar{\omega}_{QG}$ (a) from the numerical inversions of the QG- ω equation and (b) as estimated from the approximate dry decomposition (Eq. 7) for vertical velocities at 500hPa associated with precipitation extremes in CESM-LE. Results are expressed as percentage changes relative to the historical climate and normalized by the increase in global-mean surface temperature. Masking and smoothing are as in Fig. 2.

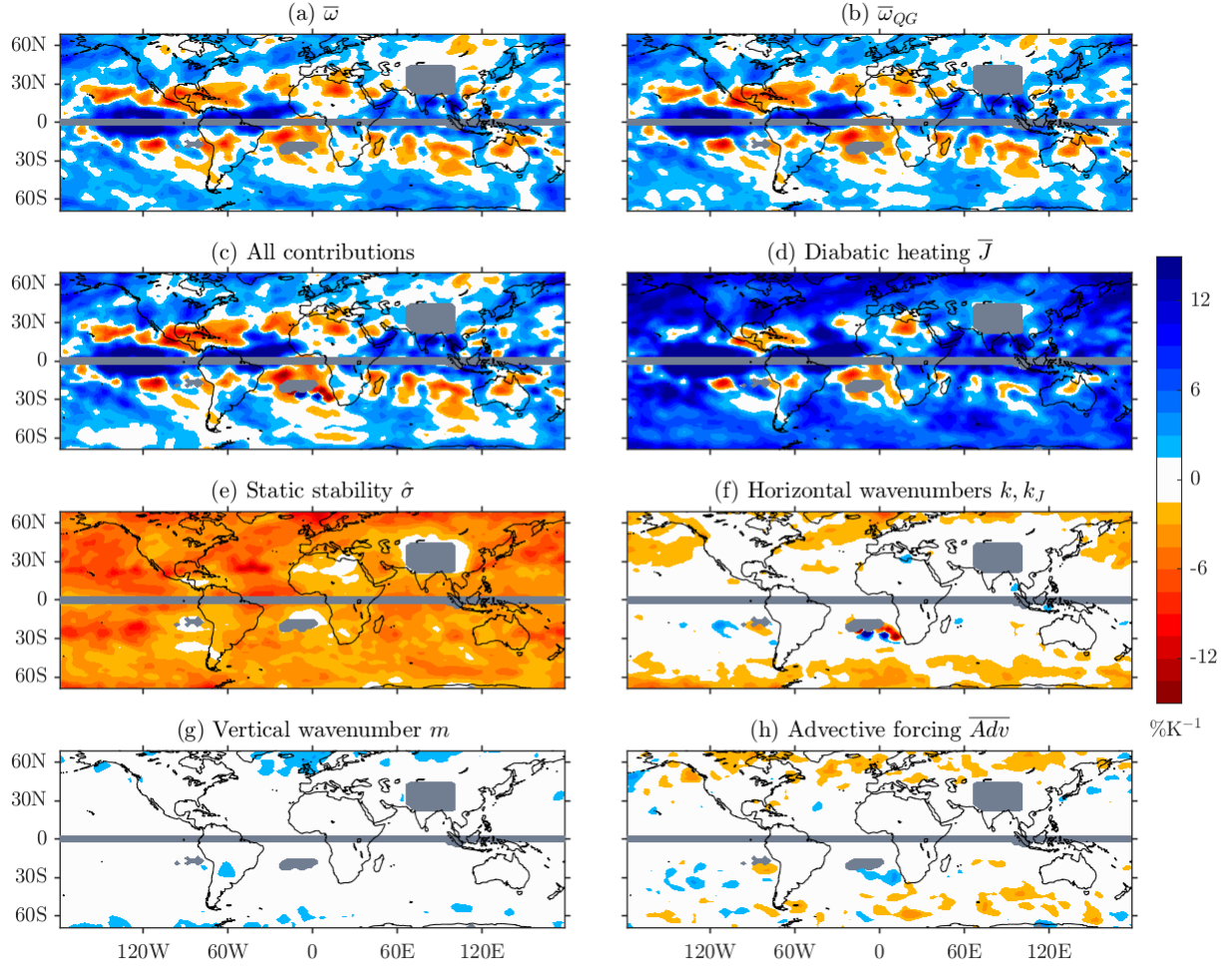


Figure S3. As in Fig. 4, but for 6-hourly events with GFDL-CM3. Grid points with fewer than 15 events are masked.

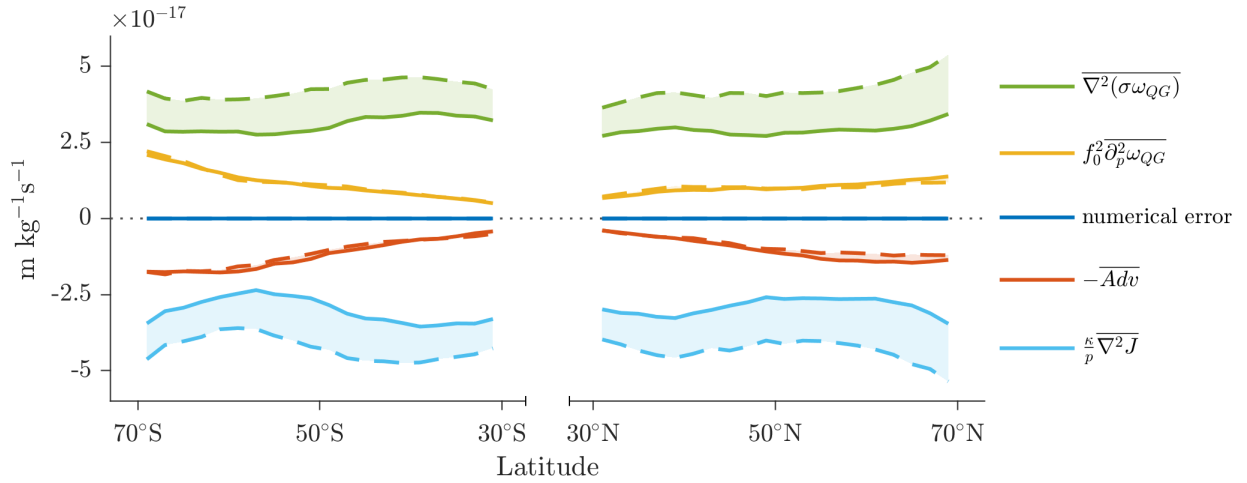


Figure S4. As in Fig. S1, but for GFDL-CM3. (Note the change of scale of the vertical axis)

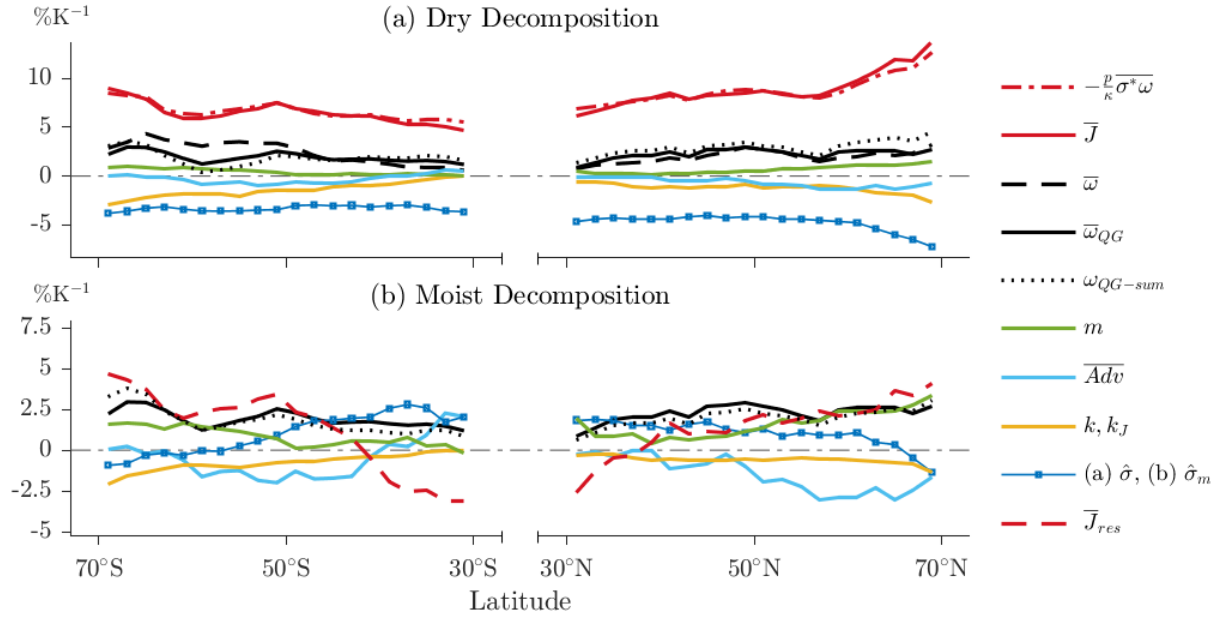


Figure S5. As in Fig. 5, but for GFDL-CM3. (Note the change of scale of the vertical axis)

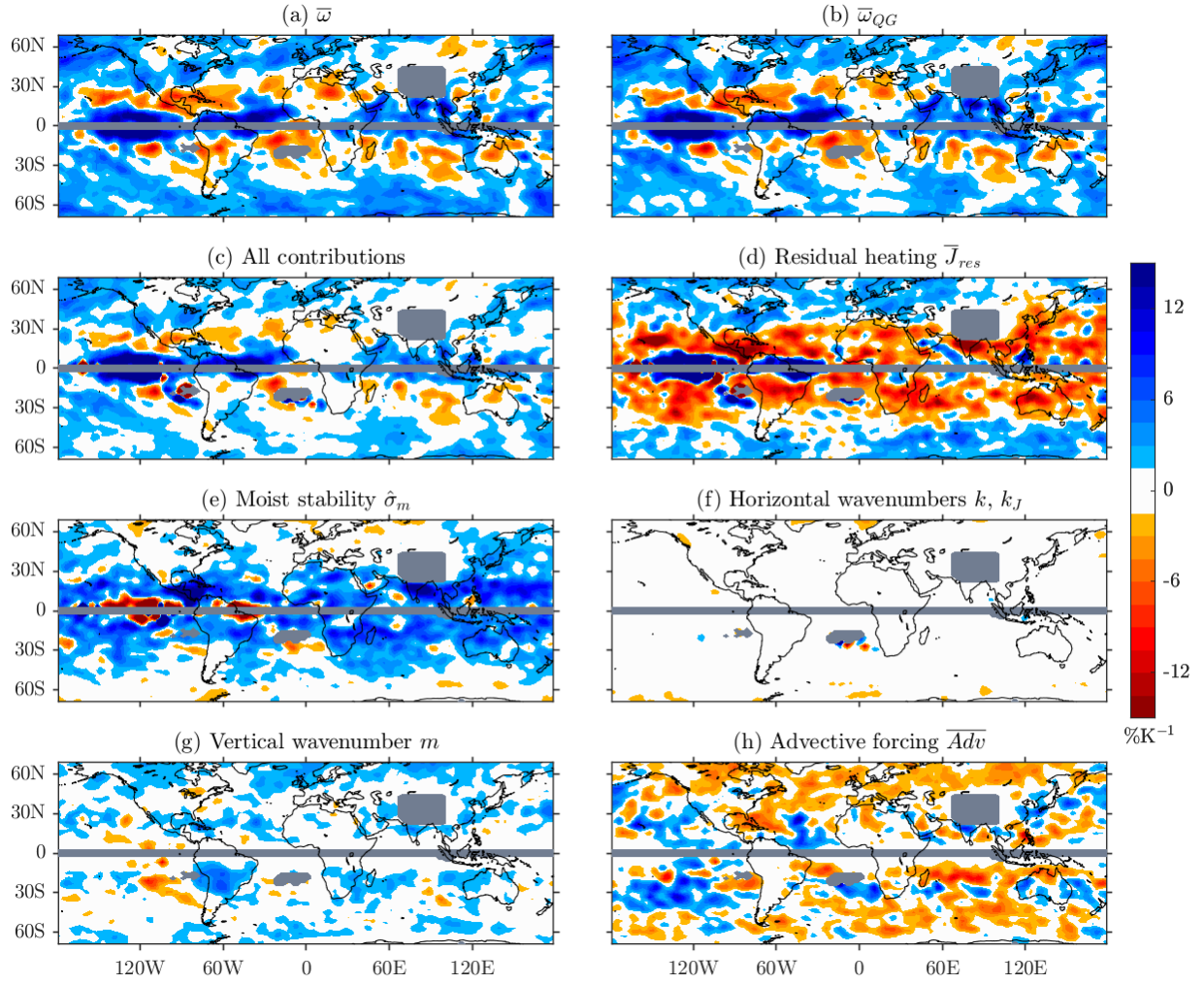


Figure S6. As in Fig. 8, but for GFDL-CM3.

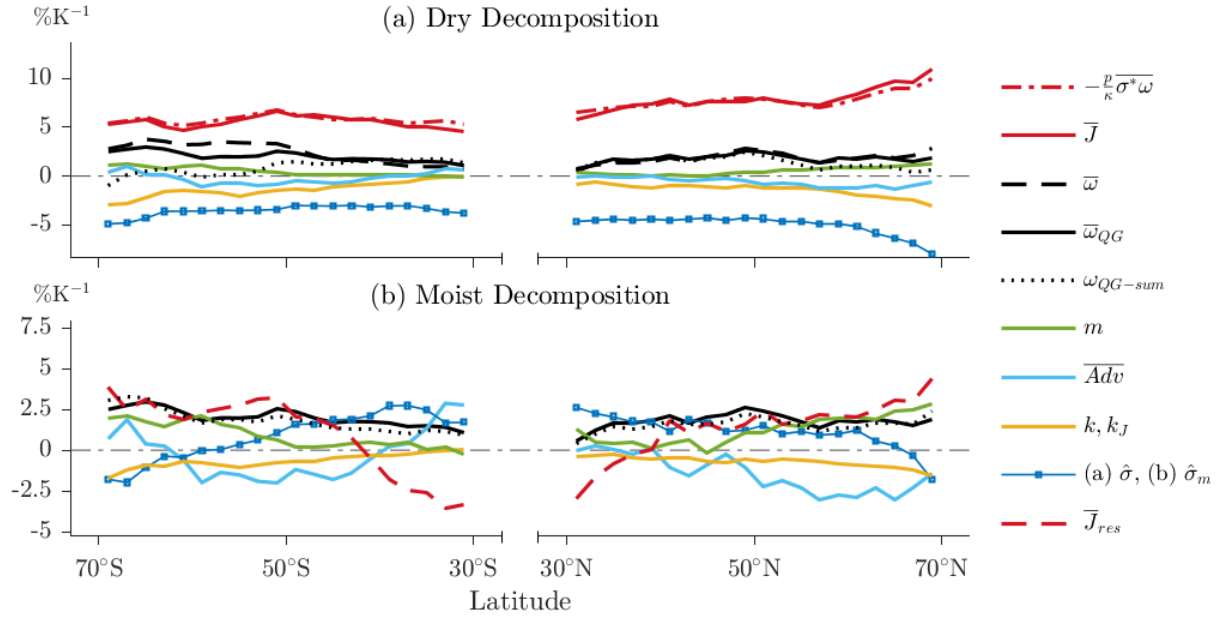


Figure S7. As in Fig. 5, but for GFDL-CM3 and the QG- ω equation is solved using ω taken from the GCM simulations for the lateral- and lower-boundary conditions.

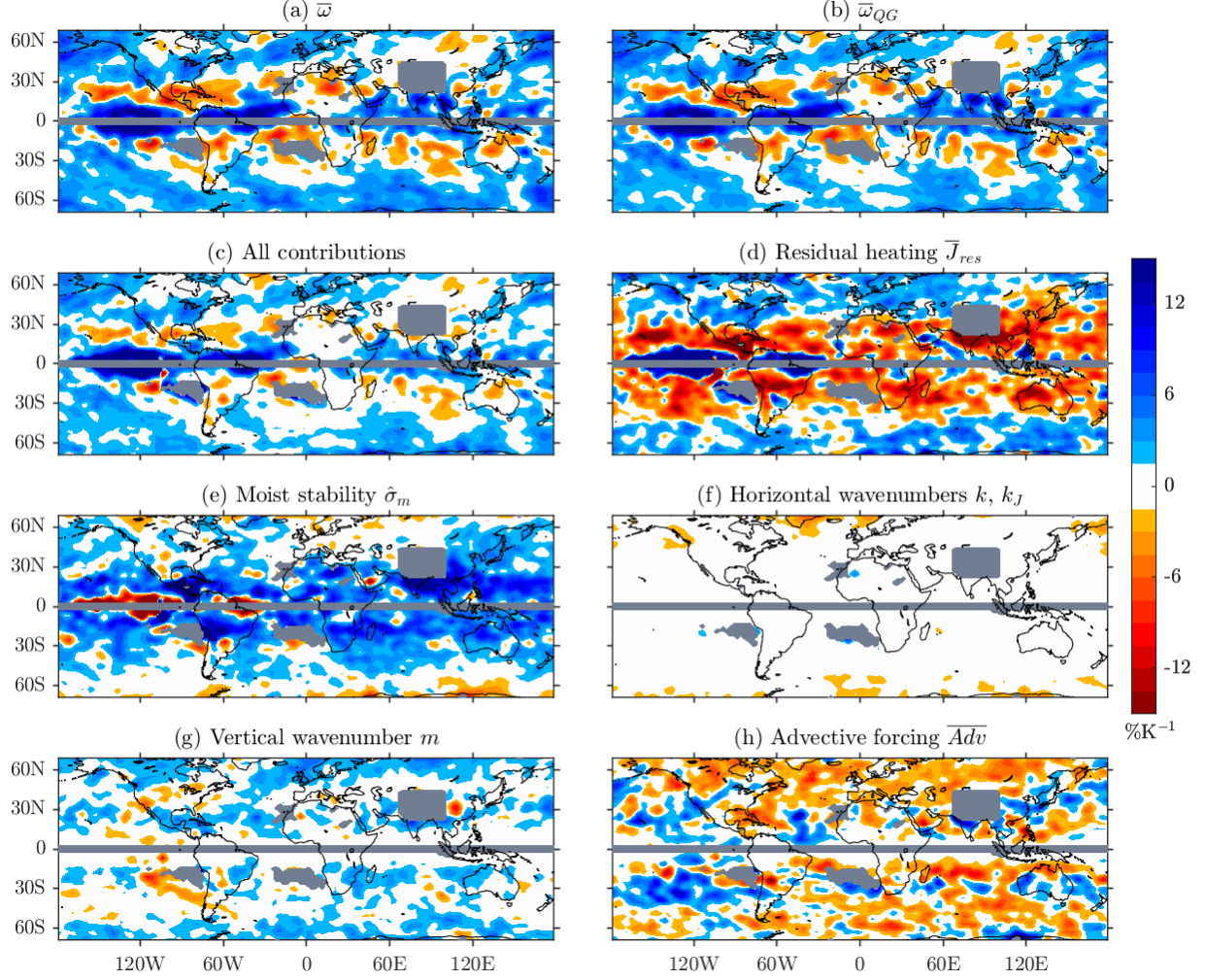


Figure S8. As in Fig. 8, but for GFDL-CM3 and the QG- ω equation is solved using ω taken from the GCM simulations for the lateral- and lower-boundary conditions.

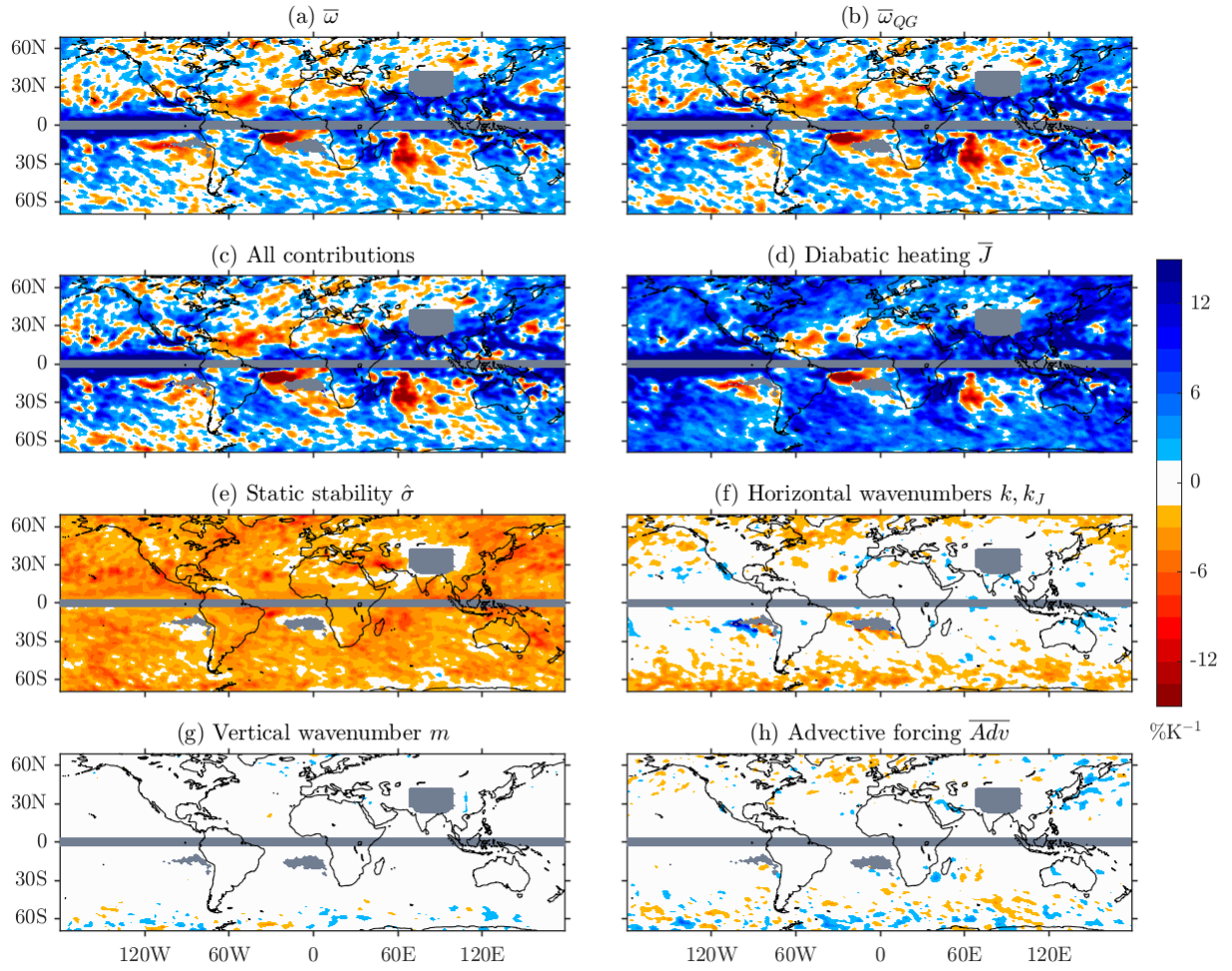


Figure S9. As in Fig. 4, but for daily precipitation extremes in CESM-LE, and grid points with fewer than 5 events are masked.

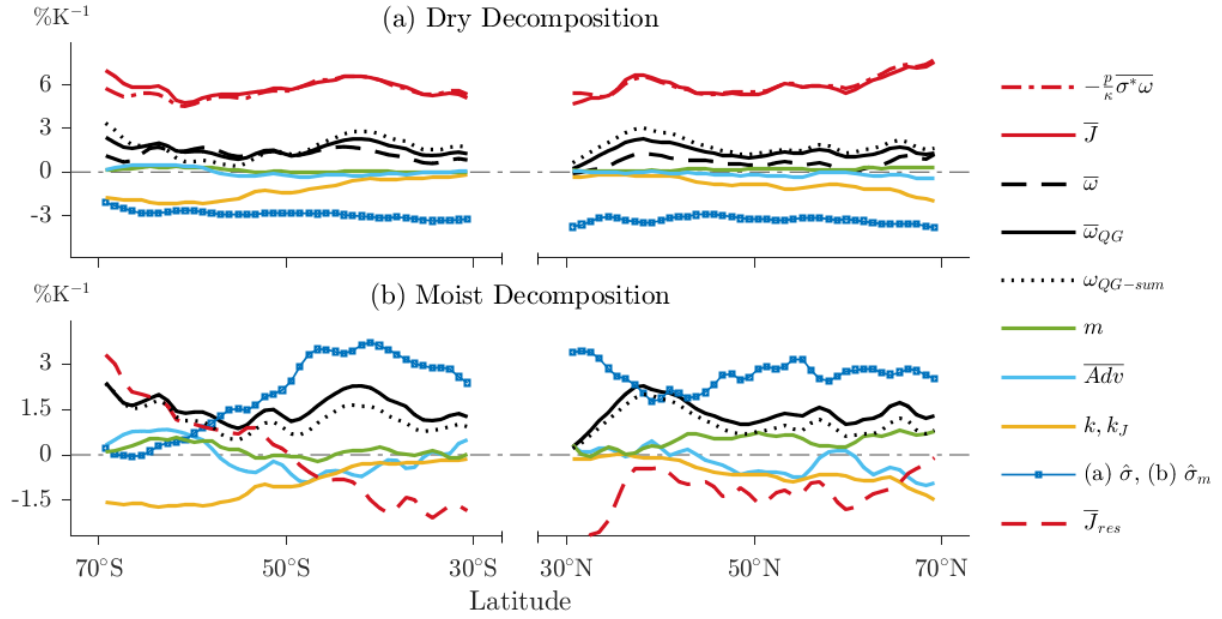


Figure S10. As in Fig. 5, but for daily precipitation extremes in CESM-LE.

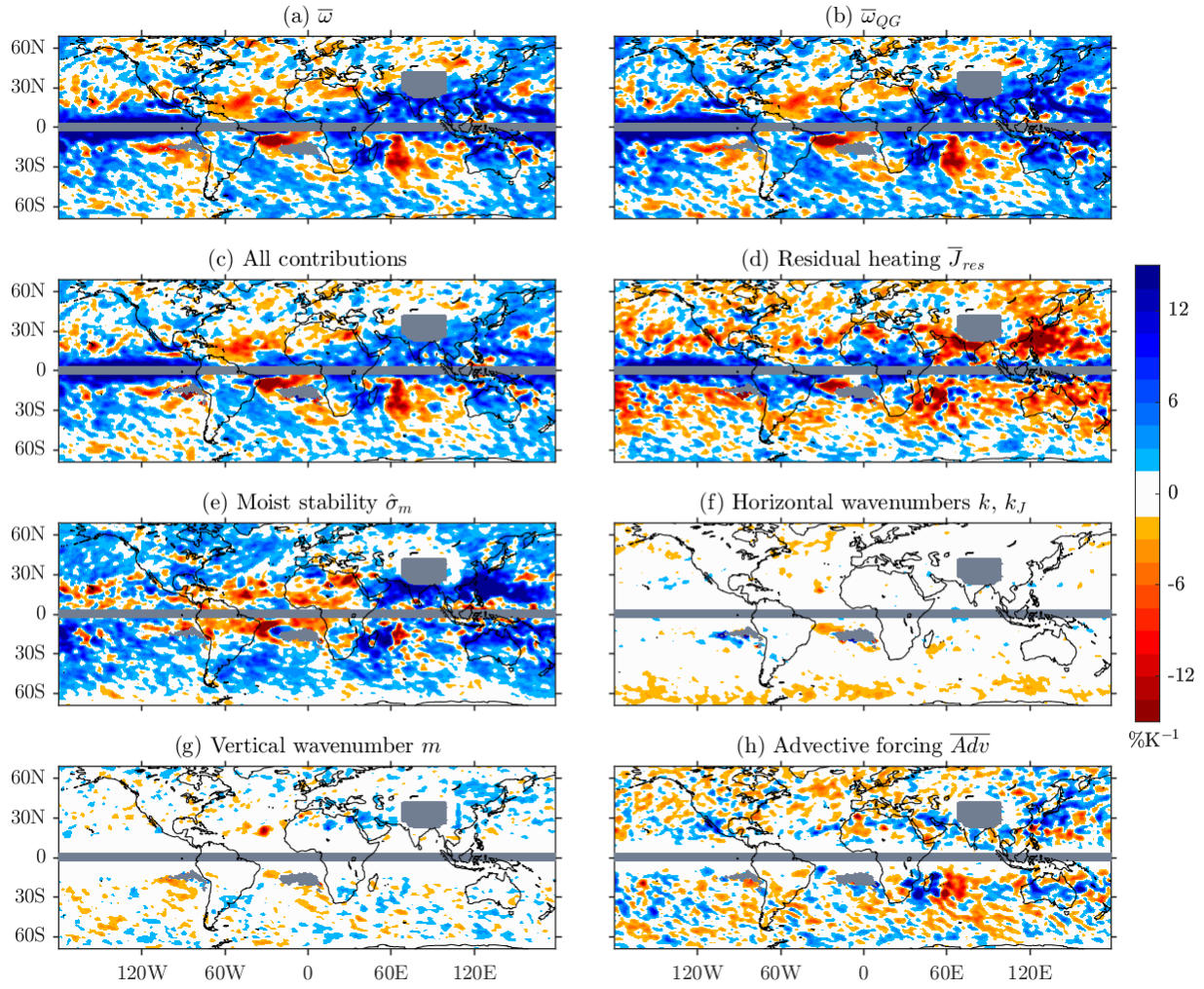


Figure S11. As in Fig. 8, but for daily precipitation extremes in CESM-LE, and grid points with fewer than 5 events are masked.

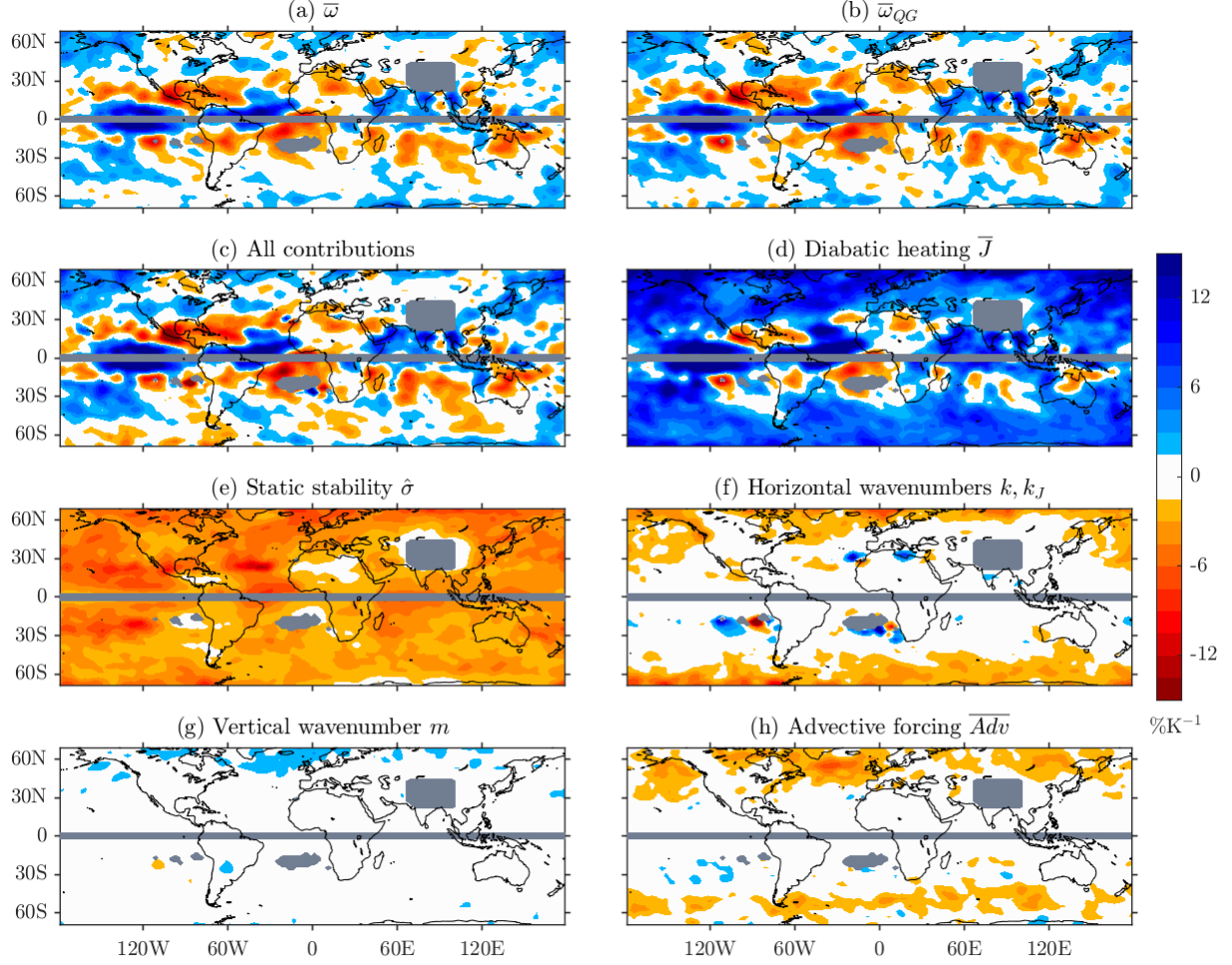


Figure S12. As in Fig. 4, but for daily precipitation extremes at the 99.5-percentile in GFDL-CM3, and grid points with fewer than 5 events are masked.

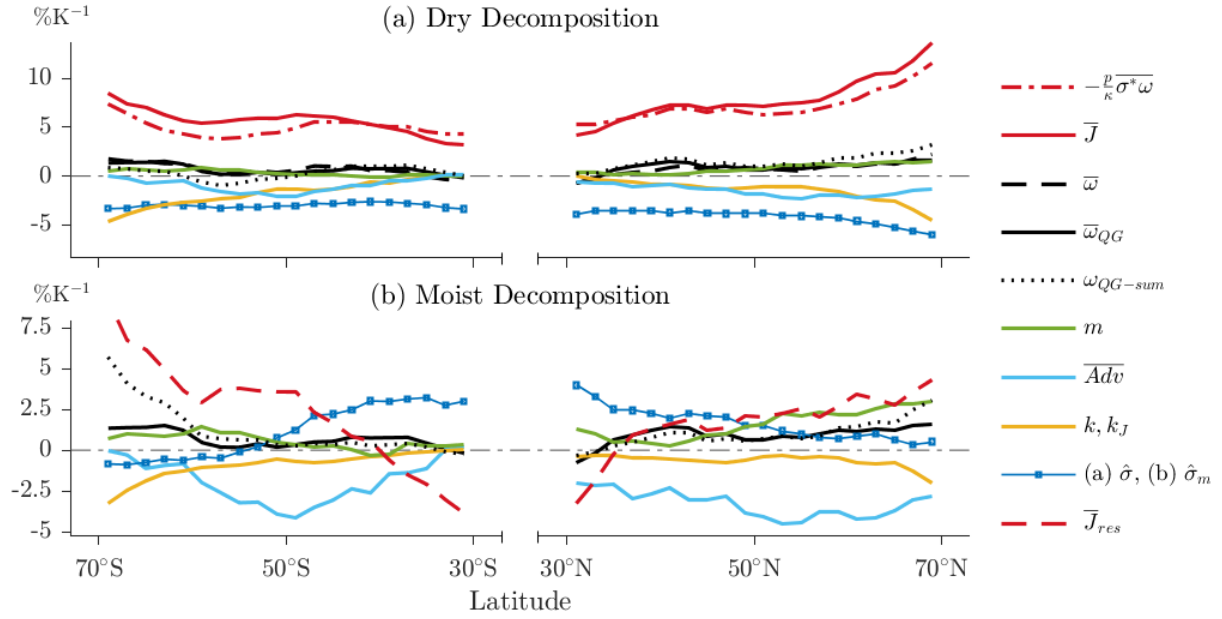


Figure S13. As in Fig. 5, but for daily precipitation extremes at the 99.5-percentile in GFDL-CM3.

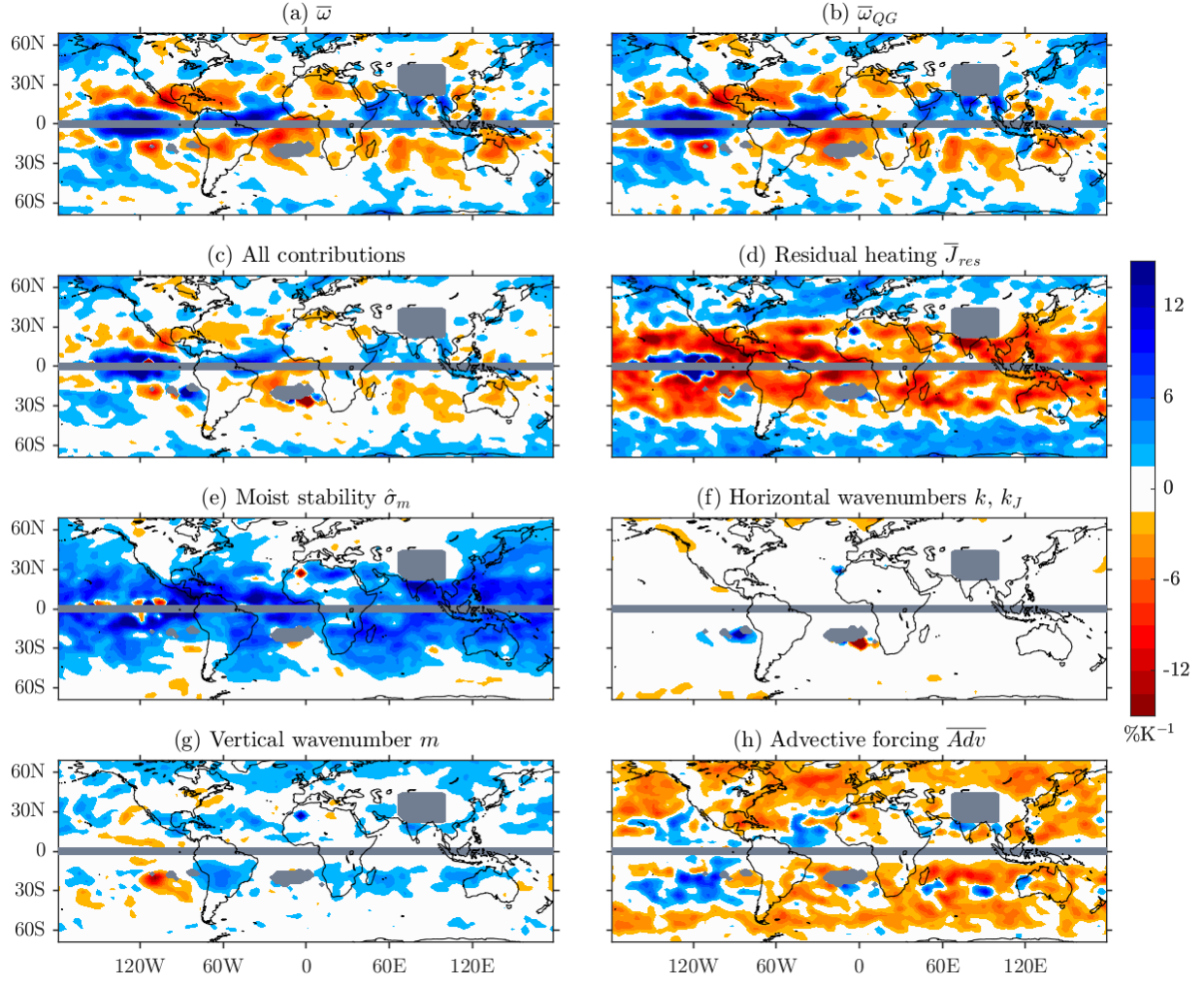


Figure S14. As in Fig. 8, but for daily precipitation extremes at the 99.5-percentile in GFDL-CM3.